Stem Cell Reports
Report

ISSCR

OPEN ACCESS

Pathological Endogenous α-Synuclein Accumulation in Oligodendrocyte Precursor Cells Potentially Induces Inclusions in Multiple System Atrophy

Seiji Kaji,[1] Takakuni Maki,[1,*] Hisanori Kinoshita,[1] Norihito Uemura,[1] Takashi Ayaki,[1] Yasuhiro Kawamoto,[1,2] Takahiro Furuta,[3] Makoto Urushitani,[4] Masato Hasegawa,[5] Yusuke Kinoshita,[6] Yuichi Ono,[6] Xiaobo Mao,[7] Tran H. Quach,[7] Kazuhiro Iwai,[8] Valina L. Dawson,[7,9,10,12] Ted M. Dawson,[7,10,11,12] and Ryosuke Takahashi[1,*]

[1]Department of Neurology, Graduate School of Medicine, Kyoto University, 54 Shogoin-Kawahara-cho, Sakyo-ku, 606-8397 Kyoto, Japan
[2]Department of Neurology, Rakusai Shimizu Hospital, Nishikyo-ku, 610-1106 Kyoto, Japan
[3]Department of Morphological Brain Science, Graduate School of Medicine, Kyoto University, Kyoto, Japan
[4]Department of Neurology, Shiga University of Medical Science, Otsu, 520-2192 Shiga, Japan
[5]Department of Dementia and Higher Brain Function, Tokyo Metropolitan Institute of Medical Science, Setagaya-ku, 156-8506 Tokyo, Japan
[6]Department of Developmental Neurobiology, KAN Research Institute, Inc., Kobe, 650-0047 Hyogo, Japan
[7]Neuroregeneration and Stem Cell Program, Institute for Cell Engineering and the Department of Neurology, Johns Hopkins University School of Medicine, Baltimore, MD 21205, USA
[8]Department of Molecular and Cellular Physiology, Graduate School of Medicine, Kyoto University, Kyoto, Japan
[9]Department of Physiology, Johns Hopkins University School of Medicine, Baltimore, MD 21205, USA
[10]Solomon H. Snyder Department of Neuroscience, Johns Hopkins University School of Medicine, Baltimore, MD 21205, USA
[11]Department of Pharmacology & Molecular Sciences, Johns Hopkins University School of Medicine, Baltimore, MD 21205, USA
[12]Adrienne Helis Malvin Medical Research Foundation, New Orleans, LA 70130-2685, USA
*Correspondence: harutoma@kuhp.kyoto-u.ac.jp (T.M.), ryosuket@kuhp.kyoto-u.ac.jp (R.T.)
https://doi.org/10.1016/j.stemcr.2017.12.001

SUMMARY

Glial cytoplasmic inclusions (GCIs), commonly observed as α-synuclein (α-syn)-positive aggregates within oligodendrocytes, are the pathological hallmark of multiple system atrophy. The origin of α-syn in GCIs is uncertain; there is little evidence of endogenous α-syn expression in oligodendrocyte lineage cells, oligodendrocyte precursor cells (OPCs), and mature oligodendrocytes (OLGs). Here, based on *in vitro* analysis using primary rat cell cultures, we elucidated that preformed fibrils (PFFs) generated from recombinant human α-syn trigger multimerization and an upsurge of endogenous α-syn in OPCs, which is attributable to insufficient autophagic proteolysis. RNA-seq analysis of OPCs revealed that α-syn PFFs interfered with the expression of proteins associated with neuromodulation and myelination. Furthermore, we detected cytoplasmic α-syn inclusions in OLGs through differentiation of OPCs pre-incubated with PFFs. Overall, our findings suggest the possibility of endogenous α-syn accumulation in OPCs that contributes to GCI formation and perturbation of neuronal/glial support in multiple system atrophy brains.

INTRODUCTION

Multiple system atrophy (MSA) is an α-synucleinopathy characterized by a relentless worsening of motor and non-motor symptoms during a typical time frame of 6–10 years. Glial cytoplasmic inclusions (GCIs) in oligodendrocytes (OLGs), which consist of α-synuclein (α-syn)-positive filamentous components, are the hallmark for a definitive neuropathological diagnosis of MSA. Given that the emergence of GCIs occurs prior to neuronal loss, it is likely that a primary oligodendroglial event is the root of the disease pathology in MSA (Wenning et al., 2008).

Since α-syn is considered to be expressed almost exclusively in neurons, the origin of the α-syn that composes GCIs in oligodendrocytes has been enigmatic. Recent reports have suggested the existence of endogenous α-syn in oligodendrocyte lineage cells, emphasizing the pathological importance of endogenous α-syn as the source of the misfolded α-syn in GCIs (Djelloul et al., 2015). The fibrillary form of α-syn contributes to prion-like propagation of the misfolded structure and disease progression among both *in vitro* and *in vivo* models of synucleinopathies (Angot et al., 2010). Considering that exogenous α-syn preformed fibrils (PFFs) seed and recruit endogenous α-syn to form insoluble aggregates in primary neurons, it is of great importance to determine if exogenous α-syn PFFs induce misfolding of endogenous α-syn in primary oligodendrocyte lineage cells (Volpicelli-Daley et al., 2011).

Oligodendrocyte lineage cells support neuronal activity not only by forming a myelin sheath to enable saltatory conduction but also by modulating axonal and neuronal homeostasis through the supply of neurotrophic factors (Wilkins et al., 2003). Myelin-forming mature OLGs are derived from oligodendrocyte precursor cells (OPCs). When activated in response to brain damage, OPCs proliferate and attempt to differentiate into mature OLGs. OPCs, which are immunoreactive to NG2 chondroitin sulfate or platelet-derived growth factor α receptor (PDGFRα), are distributed diffusely within the central nervous system and account for 5%–8% of all cells in adult brains (Levine et al., 2001). Despite the importance of OPCs in brain homeostasis, there are limited numbers of pathological investigations of OPCs in MSA brains.

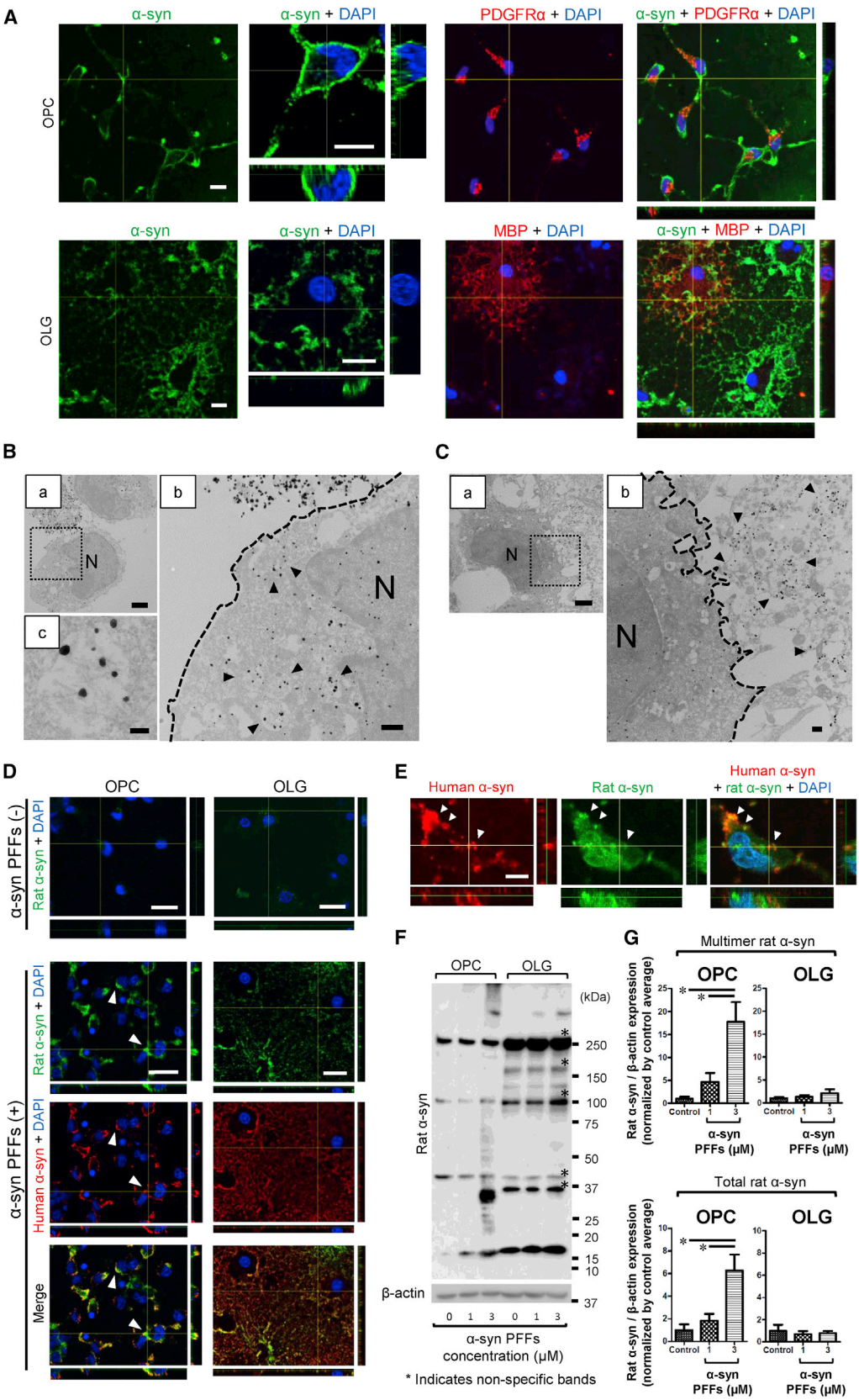

(legend on next page)

In the present study, we provide new pathological insight into the interaction between endogenous and exogenous α-syn by using primary rat oligodendrocyte lineage cell cultures, and we propose the possibility of OPC involvement in the pathogenesis of MSA.

RESULTS

Oligodendrocyte Precursor Cells Contain α-Syn Aggregates in MSA Brains

We investigated whether OPCs contain α-syn aggregates in MSA brains. One previous analysis revealed that a small fraction of OPCs in MSA cases showed α-syn immunoreactivity, which was also confirmed by our postmortem investigation (May et al., 2014) (Figure S1A). The α-syn immunoreactivity in OPCs was stained with Thioflavin S, suggesting that the α-syn aggregate was misfolded. These results suggest that not only OLGs but OPCs may also contain α-syn aggregates in MSA brains.

Oligodendrocyte Lineage Cells in Rat Primary Cultures Express Moderate Amounts of α-Syn

To confirm the endogenous α-syn expression in oligodendrocyte lineage cells, primary oligodendrocyte lineage cell cultures were obtained from neonatal rats. Consistent with previous reports, anti-α-syn antibody immunostained endogenous α-syn within OPCs and OLGs with cytoplasmic predominance (Figures S1B and S1C) (Richter-Landsberg et al., 2000). Immunoblot analysis showed that oligodendroglial endogenous α-syn expression at 4–6 days after plating was slightly greater than 20% of the neuronal α-syn expression (Figures S1D and S1E). Consistent with immunoblot analysis, quantitative real-time PCR (qPCR) also suggested that oligodendrocyte lineage cells expressed 10%–20% of the amount of α-syn transcripts expressed in neurons (Figure S1F). Immunoblot analysis, immunocytochemistry, and qPCR analysis using each cell marker validated the high purity of each cell-type culture (Figures S1D and S1G–S1I, and Movies S1 and S2).

Exogenous α-Syn PFFs Are Internalized into OPCs

To elucidate the impact of extracellular α-syn PFFs on primary oligodendrocyte lineage cells, these cells were incubated with either recombinant human α-syn PFFs or monomer for 24 hr and immunostained with an anti-α-syn antibody. When OPCs and OLGs were incubated with α-syn PFFs, prominent α-syn immunoreactivity was observed on the cell membranes. Observation of the magnified images obtained by confocal microscopy enabled visualization of internalization of α-syn predominantly in OPCs but not in OLGs (Figure 1A), which was also confirmed by immunoelectron microscopy showing the intracellular localization of α-syn fibrils in OPCs (Figures 1B and 1C). Meanwhile, the enhanced α-syn immunoreactivity was not found either in OPCs or OLGs exposed to an equivalent amount of α-syn monomer (Figure S2A). The cytosolic localization of exogenous α-syn in OPCs was also verified by subcellular fractionation of these cells (Figure S2B).

Endogenous α-Syn Protein Expression in OPCs Dramatically Increases in Response to Exogenous Recombinant Human α-Syn PFFs

To visualize the interaction between exogenous human α-syn and endogenous rat α-syn in OPCs and OLGs, cells were immunostained with an anti-α-syn antibody that specifically recognizes rodent α-syn (endogenous α-syn

Figure 1. Internalization of Recombinant Human α-Syn PFFs Inducing Accumulation and Multimerization of Endogenous Rat α-Syn

(A) Confocal microscopy of OPCs and OLGs incubated with α-syn PFFs (3 μM) shows prominent α-syn accumulation on the cell membranes. The magnified view of an OPC reveals intracellular α-syn immunoreactivity, which is not observed in OLGs. Each scale bar represents 10 μm.

(B) Immunoelectron microscopy of α-syn PFF (1 μM)-treated OPCs reveals intracellular fibril-like structures, which are labeled with anti-α-syn antibody (arrowheads). The antibody recognizes both rat and human α-syn. Each scale bar represents (a) 2 μm, (b) 500 nm, and (c) 100 nm, respectively. (b) Dotted line indicates cell surface. N, nucleus.

(C) Immunoelectron microscopy of α-syn PFF (1 μM)-treated OLGs shows extracellularly distributed layers of fibril-like structures, which are labeled with anti-α-syn antibody (arrowheads). The antibody recognizes both rat and human α-syn. Each scale bar represents (a) 2 μm and (b) 500 nm, respectively. (b) Dotted line indicates cell surface. N, nucleus.

(D) Confocal microscopy with human-specific (exogenous) and rat-specific (endogenous) anti-α-syn antibodies identifies the enhanced expression of endogenous α-syn in α-syn PFF (3 μM)-treated OPCs. The increase in rat-specific α-syn expression is less notable in OLGs treated with α-syn PFFs (3 μM). White arrowheads indicate locations where endogenous rat α-syn accumulation is predominantly observed. Each scale bar represents 20 μm.

(E) The magnified view of α-syn PFF (1 μM)-treated OPCs shows intracellular colocalization of exogenous human and endogenous rat α-syn (white arrowheads). The bar represents 5 μm.

(F) Immunoblot analysis with a rat-specific anti-α-syn antibody reveals that 24-hr incubation with α-syn PFFs induces multimerization of endogenous rat α-syn, with a remarkable increase in the total amount of endogenous rat α-syn in OPCs.

(G) Quantification of endogenous rat α-syn accumulation in α-syn PFF-treated OPCs and OLGs by immunoblot analysis is illustrated. Both total and multimer endogenous rat α-syn are significantly increased in OPCs by α-syn PFF application. Mean ± SEM; n = 5, respectively, independent cultures; one-way ANOVA, *$p < 0.05$.

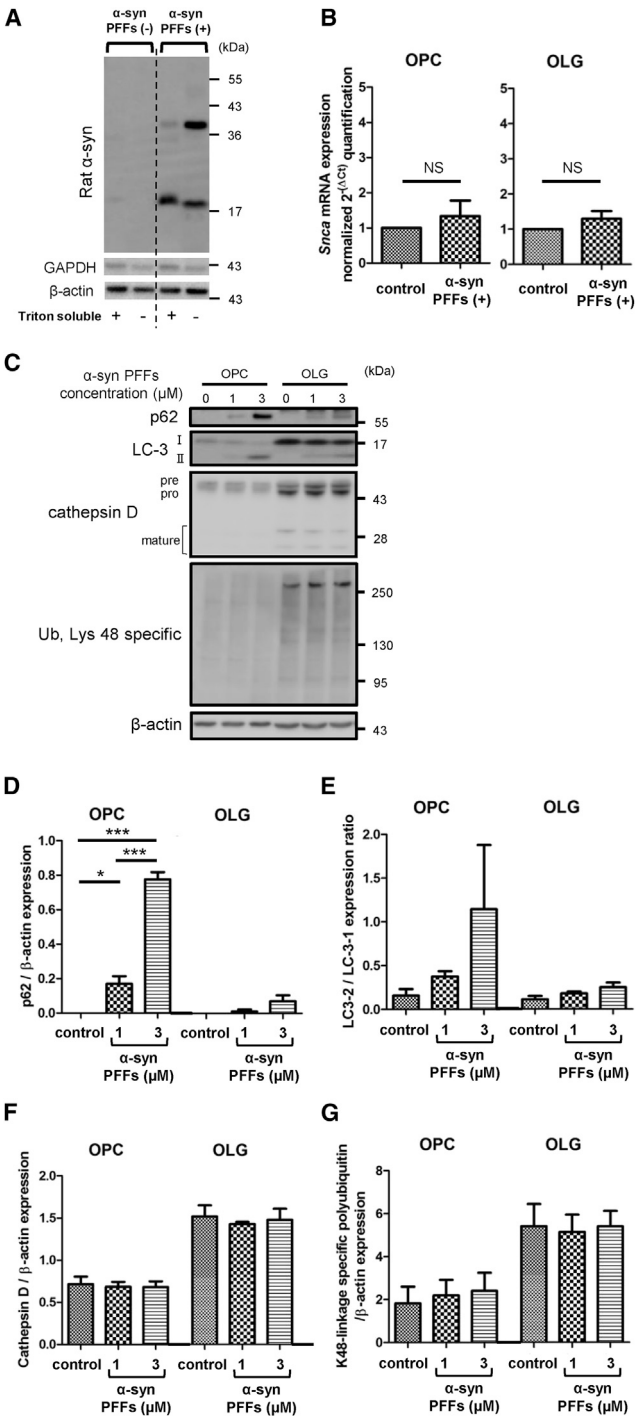

Figure 2. Insufficient Autophagic Degradation in OPCs Triggered by α-Syn PFF Application

(A) Accumulation of Triton-insoluble endogenous rat α-syn in OPCs is triggered by α-syn PFF (3 μM) application.

(B) Quantitative real-time PCR reveals unchanged *Snca* expression levels after 72-hr incubation of oligodendrocyte lineage cells with 3 μM α-syn PFFs. Mean ± SEM; n = 6, respectively, independent cultures; paired t test. NS, not statistically significant.

(C) Immunoblot analysis with proteolytic markers discloses marked increases in p62 and LC3-II in OPCs, suggesting the induction of an autophagic pathway due to α-syn PFF application.

(D–G) Quantification of each proteolytic marker expression in oligodendrocyte lineage cell is exhibited. (D and E) Autophagic indicators, p62 and LC3-II/LC3-I, show increasing trends in α-syn PFF-treated OPCs. (F) Cathepsin D protein expression is not significantly affected by α-syn PFF application. (G) The expression of lysine-48-linked ubiquitin chains is not affected by α-syn PFF application. Mean ± SEM; n = 4, respectively, independent cultures; one-way ANOVA, *p < 0.05, ***p < 0.001.

antibody) (Figure S2C). In response to incubation with exogenous α-syn PFFs, the endogenous α-syn expressions in OPCs were remarkably enhanced (Figures 1D and S2D). The enhanced immunoreactivity of endogenous α-syn colocalized with that of exogenous α-syn in the cytoplasm of OPCs (Figures 1E and S2B). The cytoplasmic inclusions immunostained with the endogenous α-syn antibody were also stained with Thioflavin S, which was exclusively observed in OPCs (Figures S2E and S2F). Immunoblot analysis revealed a drastically increased amount of endogenous α-syn expression in OPCs characterized by the emergence of multimerized α-syn as the result of α-syn PFF application (Figures 1F and 1G). On the other hand, there was minimal change in the total amount of endogenous α-syn expression in OLGs, as shown by both immunostaining and immunoblot analysis. Monomeric α-syn did not alter the protein expression pattern of endogenous α-syn in OPCs (Figure S2G). Despite the striking evidence of inclusion formation in OPCs, the expression of phosphorylated α-syn was not confirmed either in immunostaining or immunoblot analysis (Figures S2H and S2I).

Impairment of Autophagy Contributes to Endogenous α-Syn Accumulation in OPCs

Incubation of OPCs with α-syn PFFs facilitated expression of endogenous α-syn not only in Triton-soluble fractions but also in Triton-insoluble fractions (Figure 2A). Based on the evidence of pathological α-syn expression, we then asked whether the endogenous α-syn protein increase is caused by overproduction, accompanied by increased α-syn transcripts, or by proteolytic dysfunction. qPCR of oligodendrocyte lineage cells 72 hr after application of α-syn PFFs clarified that there was no significant increase in α-syn transcripts (Figure 2B).

Subsequently, we investigated the effect of 24-hr application of α-syn PFFs on proteolytic systems in oligodendrocyte lineage cells. Immunoblot analysis of α-syn PFF-treated cells revealed p62 accumulation and fraction conversion of LC3-I to LC3-II in OPCs (Figures 2C and 2E), which are correlated with insufficient autophagic clearance and autophagosome accumulation, respectively.

These findings, as well as the increase of endogenous α-syn, were also observed when OPCs were incubated for 24 hr with an autophagy inhibitor, chloroquine (Figures S3A–S3C). The interaction of α-syn and autophagy markers (p62, Beclin-1, and LC3) as well as the intra-lysosomal localization of α-syn was verified by immunostaining and LysoTracker probes, implying the possibility of compromised lysosomal degradation (Figures S3D and S3E). Conversely, the protein expression levels of p62 and LC3-II in OLGs treated with α-syn PFFs only slightly increased, which did not reach statistical significance.

Cathepsin D is one of the lysosomal enzymes that are known to regulate cell homeostasis by mediating the degradation of misfolded protein aggregates delivered to lysosomes via autophagy or endocytosis (Bae et al., 2015). Although the α-syn PFF application did not affect the cathepsin D protein expression levels in OPCs or OLGs, the enzymatic activity analysis suggested the reduced cathepsin D activity in α-syn PFF-treated OPCs (Figures 2C, 2F, and S3F).

Lysine-48-linked polyubiquitin chains are well established as the signal for 26S proteasomal degradation (Grice and Nathan, 2016). Both the OPCs and OLGs showed no appreciable increase in lysine-48-linked ubiquitin chains (Figures 2C and 2G). Taken together, these results indicate that α-syn PFFs impair autophagy more severely in OPCs compared with OLGs, leading to the accumulation of endogenous α-syn proteins.

α-Syn PFFs Interfere with mRNA Expression Related to Myelination and Neuronal Support in Oligodendrocyte Precursor Cells

Media lactate dehydrogenase (LDH) and water-soluble tetrazolium (WST) assays revealed that α-syn PFFs did not cause acute cell death after 24-hr exposure (Figures S3G and S3H). Therefore, we assessed the functional influence of α-syn PFF application on OPCs.

RNA sequencing (RNA-seq) analysis in OPCs revealed remarkable alterations in mRNA profiles associated with OLG maturation and neuromodulation after 72-hr α-syn PFF application (Figure 3A). As for the gene expression involved in oligodendrocyte maturation, α-syn PFF application to OPCs suppressed the gene expressions of myelination-promoting factors such as *Ackr3* (encoding CXCR-7) and *Cntn1* (encoding Contactin 1), while increasing those of myelination-inhibiting factors such as *Sirt2* (encoding sirtuin 2) and *Il1b* (interleukin 1β). Among the neurotrophic factors that regulate neurodegenerative disease pathology, monocarboxylate transporter 1 (MCT1) encoded by *Slc16a1*, which mediates neuronal death through the release of lactate, and brain-derived neurotrophic factor (BDNF) showed a tendency to decrease (Lee et al., 2012). Therefore, we verified the alteration of mRNA expression levels of *Slc16a1* and *Bdnf* (Figures 3B and 3C) as well as those of glial cell-derived neurotrophic factor (*Gdnf*) and insulin-like growth factor-1 (*Igf1*) by qPCR (Figures S3I and S3J). Interestingly, the mRNA expression level of *Slc16a1* was significantly suppressed, whereas those of *Bdnf* and *Gdnf* were unchanged. The perturbation of these neurotrophic factors induced by extracellular α-syn PFFs was more severe in OPCs than in OLGs, possibly reflecting the difference of α-syn internalization and susceptibility against seeding. Alterations of mRNA expression levels were observed in various profiles associated with proteolysis and protein trafficking (Figure S3K), phenotypic markers (Figure S3L), and risk genes for familial Parkinson's disease and MSA (Figure S3M). The results and interpretation of RNA-seq analysis regarding possible endocytic players for α-syn PFF uptake in OPCs are described in the Supplemental Information.

OPCs Pre-incubated with Recombinant Human α-Syn PFFs Differentiate into Mature OLGs with Endogenous α-Syn-Positive Inclusions

To determine if the endogenous α-syn accumulation in OPCs remains even after differentiation into mature OLGs, we tried to differentiate α-syn PFFs-treated OPCs according to the procedure shown in Figure 4A. Immunostaining revealed α-syn aggregates in differentiated OLGs, which were also immunoreactive to an endogenous α-syn antibody (Figures 4B–4D). Immunoelectron microscopy showed the intracellular existence of fibrillar α-syn (Figure S4A). An anti-phosphorylated α-syn antibody detected vague immunoreactivity merged with α-syn aggregates through immunostaining, nevertheless the immunoreactivity was not detectable with immunoblot analysis (Figures S4B and S4C). Pre-incubation with α-syn PFFs also caused a reduction in myelin-associated proteins, such as myelin basic protein (MBP) and tubulin polymerization promoting protein (TPPP/p25α) (Figures 4E, S4D, and S4E). The decrease of these OLG-specific markers was accompanied with an increase in the protein expression levels of PDGFRα and a decreasing trend of *Mbp* mRNA expression levels, suggesting insufficient differentiation as a result of α-syn PFF application (Figures S4F–S4I).

In order to delineate the functional consequence induced by α-syn PFF application before maturation, we focused on the neuro-supportive function of conditioned medium from OLGs (Figures 4F–4I). The equivalent medium kept under the same conditions in culture flasks without cells was used as control medium. Generally, when primary neurons are incubated with full-medium change, the survival of neurons is impaired compared with half-medium change. The conditioned medium from our OLG culture promoted the survival of primary neurons even with full-medium change. Notably, this

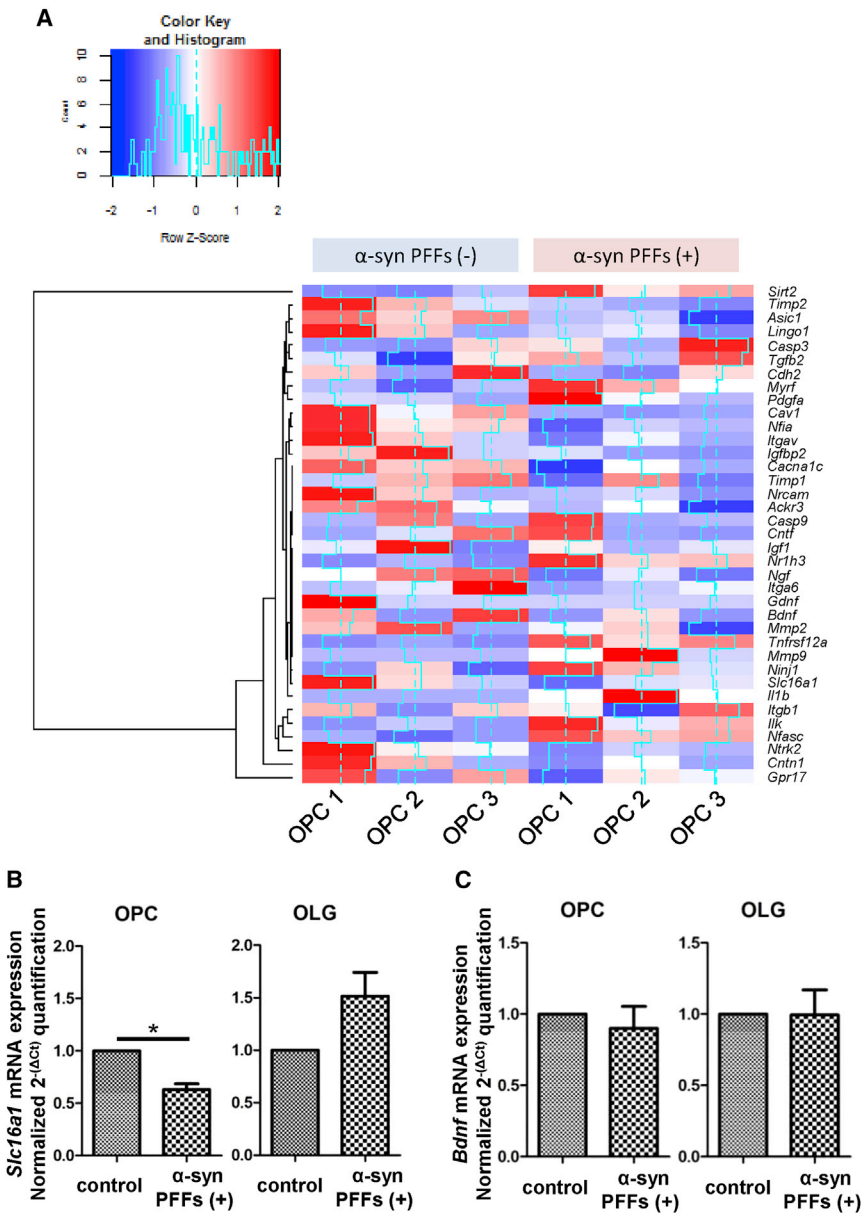

Figure 3. RNA-Seq and qPCR Analysis for mRNA Expression Alteration in α-Syn PFF-treated OPCs

(A) RNA-seq analysis of α-syn PFF-treated OPCs discloses a dramatic shift in the expression of transcripts related to neuromodulation, myelination, and cell survival. Each pair of OPC culture samples (OPC1, OPC2, and OPC3) was allocated for the two groups with and without α-syn PFF (3 μM) application.

(B and C) qPCR elucidates reduced mRNA expression of *Slc16a1* in α-syn PFF (3 μM)-treated OPCs, whereas *Bdnf* mRNA expression is not significantly affected. Mean ± SEM; n = 6, respectively; independent cultures; paired t test, *p < 0.05.

neuro-supportive effect was suppressed when OLGs were differentiated from OPCs pretreated with α-syn PFFs.

DISCUSSION

The existence of endogenous α-syn in primary oligodendroglial cell culture has been previously reported by Richter-Landsberg et al. (2000). On the other hand, a previous report of *in situ* hybridization in GCI-rich regions revealed no increase in α-syn mRNA expression in MSA brains compared with controls (Miller et al., 2005). The *in vitro* findings of endogenous α-syn accumulation as a reflection of autophagic impairment in oligodendrocyte lineage cells in our study (Figures 1D–1G) are in keeping with both of the previous studies and suggested the possibility that endogenous α-syn in oligodendrocyte lineage cells per se contributes to the formation of α-syn aggregates in MSA.

Macroautophagy is particularly important for pathological α-syn clearance, as it can degrade insoluble or aggregated forms of proteins (Konno et al., 2012). In fact, GCIs in MSA brains are immunoreactive to autophagic markers, such as LC-3 and p62 (Schwarz et al., 2012). In addition, the downregulation of a lysosomal enzyme, cathepsin D, is associated with intracellular α-syn accumulation in

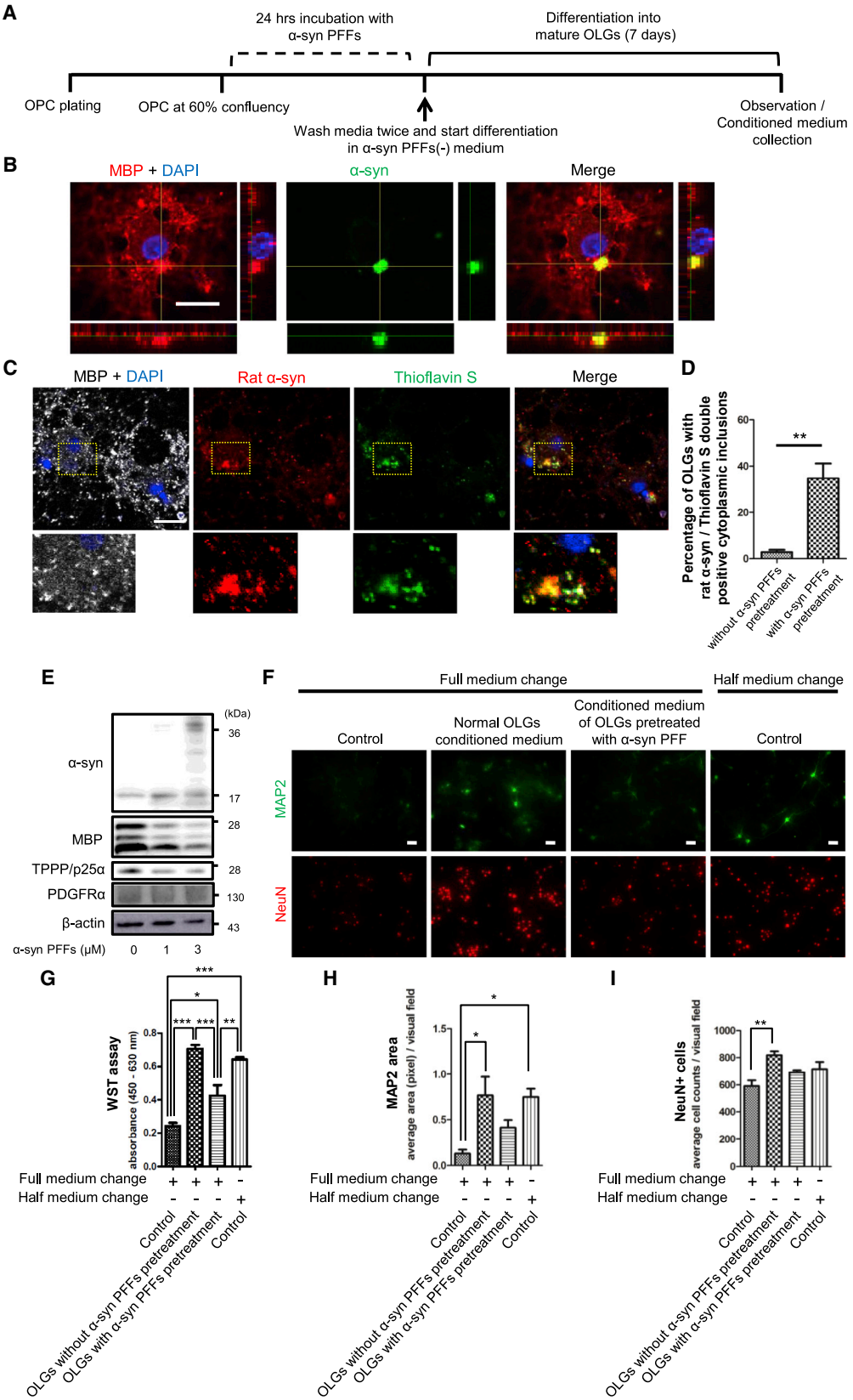

(legend on next page)

SH-SY5Y cells and myelin degeneration in knockout mice (Mutka et al., 2010; Bae et al., 2015). The lysosomal localization of α-syn, as well as the altered cathepsin D activity in OPCs of our study, emphasizes the pathological relevance of insufficient lysosomal degradation for α-syn accumulation and disease progression in MSA patients (Figures S3E and S3F).

Loss of neurotrophic support from oligodendrocytes in MSA has been postulated as the mechanism for neurodegeneration secondary to the primary glial pathology (Fellner et al., 2011). The RNA-seq and qPCR analysis corroborated that OPCs express comparable amounts of transcripts related to neuro-supportive factors, such as MCT1, BDNF, and GDNF (Figures S1H and 3). The lack of metabolic support for neurons by oligodendroglial MCT-1, a key player for the shuttling of lactate, results in neuronal death, which potentially contributes to neuronal degeneration in MSA (Lee et al., 2012). Furthermore, the OLGs containing α-syn aggregates in our experiments showed decreased expression levels of myelin-associated proteins and compromised neuro-supportive function via soluble factors (Figures 4E–4I). These findings are consistent with a previous investigation that detected myelin loss and neurodegeneration in the brains of transgenic MSA mice overexpressing α-syn in OLGs (Shults et al., 2005).

A limitation of the present study is that primary oligodendrocyte lineage cell cultures can only be used in experiments with relatively short incubation times due to the short survival time of these cells. Thus, we conducted the studies with higher concentrations of recombinant human α-syn PFFs compared with the concentrations used in the previous study of primary neurons (Volpicelli-Daley et al., 2011). In consequence, our study could not clearly detect phosphorylated α-syn immunoreactivity in oligodendroglial cells, even with 7 days of incubation after α-syn PFF administration (Figures S2H, S2I, S4B, and S4C). Considering that at least 7–10 days of the incubation period is required for neuronal α-syn to be phosphorylated, a longer observation period is warranted to confirm phosphorylation of α-syn in oligodendrocyte lineage cells with their modest basal α-syn expression compared with neurons (Volpicelli-Daley et al., 2011). As another limitation of the present study, we administered α-syn PFFs to cultured OPCs and OLGs to induce endogenous α-syn aggregation, since this is the standard protocol for α-syn aggregate formation in neurons (Volpicelli-Daley et al., 2011). However, the primary pathogenesis by which oligodendrocytes specifically trigger the production of misfolded α-syn in MSA is yet to be elucidated.

Overall, *in vitro* α-syn PFF administration in our primary cultures recapitulated a critical aspect of MSA pathogenesis and thus represents a practical model system. We suggest that OPCs potentially play a role in MSA pathology through internalization of extracellular α-syn and accumulation of endogenous α-syn, and that manipulation of α-syn expression in OPCs may serve as a therapeutic strategy against GCI formation.

EXPERIMENTAL PROCEDURES

Study Approval

Autopsied human brains were obtained from Kyoto University Hospital through a process approved by an institutional research committee. All animal procedures were performed according to the guidelines of the Animal Use and Care Committee of Kyoto University and of the Institute of Biomedical Research and Innovation.

Primary Oligodendrocyte Lineage Cell Cultures

Mixed glial cell cultures were obtained from cerebral cortices of 1- to 2-day-old Sprague-Dawley rats and prepared as previously

Figure 4. Cytoplasmic α-Syn Inclusions and Impaired Neuro-supportive Function in Mature OLGs Derived through Maturation-Induction of α-Syn PFF-Treated OPCs

(A) Time chart of the experimental procedure is displayed. Cells are incubated with α-syn PFFs (1 or 3 μM) for 24 hr followed by complete removal of extracellular α-syn PFFs and initiation of 7 days of maturation.

(B) Cytoplasmic α-syn inclusion is confirmed by confocal microscopy. The scale bar represents 20 μm.

(C) The cytoplasmic inclusions contain endogenous rat α-syn. The inclusions are also labeled with Thioflavin S staining. The scale bar represents 20 μm.

(D) Percentages of OLGs containing cytoplasmic inclusions labeled with both endogenous rat α-syn and Thioflavin S are compared between OLGs with and without α-syn PFF (1 μM) pretreatment before maturation. Mean ± SEM; n = 3, respectively; independent cultures; one-way ANOVA, $^{**}p < 0.01$.

(E) Immunoblot analysis reveals reduced myelin-associated proteins, MBP and TPPP/p25α, in OLGs pretreated with α-syn PFFs before maturation.

(F) Immunostaining of primary cortical neurons incubated with conditioned medium from OLGs reveals that reduced neuronal expressions of MAP2 and NeuN are induced by α-syn PFF (3 μM) pretreatment to OPCs before maturation. Each scale bar represents 50 μm.

(G–I) Viability of primary neurons is evaluated by the quantification of (G) WST assay, (H) MAP2-positive areas, and (I) numbers of NeuN-positive cells. Mean ± SEM; n = 4, respectively; independent cultures; one-way ANOVA, $^{*}p < 0.05$, $^{**}p < 0.01$, $^{***}p < 0.001$.

described (Maki et al., 2015). Isolated OPCs were differentiated into mature OLGs by incubation with differentiation medium for 7 days.

Preparation of Recombinant Human α-Syn

Recombinant human α-syn was purified in accordance with a previously established method (Masuda-Suzukake et al., 2013). PFFs were diluted in PBS at 1 μM or 3 μM, sonicated several times (30–60 s in total), filtered with 0.2-μm syringe filters (Life Sciences), and diluted in medium.

Immunostainings Observed with Confocal Laser Microscopy

An Olympus Fluoview FV1000 confocal microscope was used to observe immunostaining with secondary antibodies conjugated to fluorescein isothiocyanate, Texas red, or Cy5 (1:200, Alexa Fluor 488, 594, and 647).

RNA-Seq Analysis of OPCs

Agilent SureSelect Strand Specific RNA prep kit (catalog no. G9691A) was used with 200 ng of total RNA to construct cDNA libraries.

Statistical Analysis

All quantitative data were analyzed by using GraphPad Prism 5.0.

ACCESSION NUMBERS

The GEO accession number for the full dataset of RNA-seq is GEO: GSE107582; see https://www.ncbi.nlm.nih.gov/geo/query/acc.cgi?acc=GSE107582 for more information and a full list of supported databases.

SUPPLEMENTAL INFORMATION

Supplemental Information includes Supplemental Experimental Procedures, four figures, one table, and two movies and can be found with this article online at https://doi.org/10.1016/j.stemcr.2017.12.001.

AUTHOR CONTRIBUTIONS

S.K., study design, data acquisition and analysis, and drafting the manuscript and figures; T.M., study conception and design, supervising the preparation of primary cultures and data acquisition, and critical revision of the manuscript; H.K., N.U., and M.H., supervising the preparation of α-synuclein; T.A. and W.K., histopathological data acquisition and analysis; T.F., supervising electron microscopic data acquisition and analysis; M.U. and K.I., study conception, data interpretation, and critical revision of the manuscript; Y.O. and Y.K., data acquisition by RNA-seq analysis; X.B.M., V.L.D., Q.T., and T.M.D., data acquisition and analysis and critical revision of the manuscript for important intellectual content; R.T., funding, supervising, and critical revision of the manuscript for important intellectual content.

ACKNOWLEDGMENTS

We thank all of our colleagues and staff at the Department of Neurology, Graduate School of Medicine, Kyoto University, including H. Yamashita, A. Kuzuya, H. Yamakado, M. Uemura, M. Hishizawa, Y. Taruno, M. Ikuno, E. Nakanishi, M. Sawamura, S. Okuda, K. Yasuda, S. Matsuzawa, Y. Hatanaka, R. Hikawa, and R. Tamano for their expert advice. We thank Dr. M. Takahashi for methodological suggestions on the immunoblot analysis. R.T. is supported by Grants-in-Aid for Scientific Research (A) (15H02540) and Grants-in-Aid for Scientific Research on Innovative Area Brain Environment (23111002) from the Japan Society for the Promotion of Science. T.M. is supported by Grants-in-Aid for Scientific Research (C) (16K07056) from the Ministry of Education, Culture, Sports, Science and Technology in Japan. X.B.M. is supported by NIH/NIA Johns Hopkins ADRC P50 AG05146. X.B.M., T.H.Q., V.L.D., and T.M.D. are supported by JPB and NIH/NINDS grant P50 NS38377. T.M.D. is the Leonard and Madlyn Abramson Professor in Neurodegenerative Diseases. X.B.M., V.L.D., and T.M.D. acknowledge the joint participation by the Adrienne Helis Malvin Medical Research Foundation through its direct engagement in the continuous active conduct of medical research in conjunction with the Johns Hopkins Hospital and the Johns Hopkins University School of Medicine and the foundation's Parkinson's Disease Program M-2014.

Received: January 17, 2017
Revised: December 2, 2017
Accepted: December 4, 2017
Published: January 11, 2018

REFERENCES

Angot, E., Steiner, J.A., Hansen, C., Li, J.Y., and Brundin, P. (2010). Are synucleinopathies prion-like disorders? Lancet Neurol. *9*, 1128–1138.

Bae, E.J., Yang, N.Y., Lee, C., Kim, S., Lee, H.J., and Lee, S.J. (2015). Haploinsufficiency of cathepsin D leads to lysosomal dysfunction and promotes cell-to-cell transmission of alpha-synuclein aggregates. Cell Death Dis. *6*, e1901.

Djelloul, M., Holmqvist, S., Boza-Serrano, A., Azevedo, C., Yeung, M.S., Goldwurm, S., Frisen, J., Deierborg, T., and Roybon, L. (2015). Alpha-synuclein expression in the oligodendrocyte lineage: an in vitro and in vivo study using rodent and human models. Stem Cell Reports *5*, 174–184.

Fellner, L., Jellinger, K.A., Wenning, G.K., and Stefanova, N. (2011). Glial dysfunction in the pathogenesis of alpha-synucleinopathies: emerging concepts. Acta Neuropathol. *121*, 675–693.

Grice, G.L., and Nathan, J.A. (2016). The recognition of ubiquitinated proteins by the proteasome. Cell. Mol. Life Sci. *73*, 3497–3506.

Konno, M., Hasegawa, T., Baba, T., Miura, E., Sugeno, N., Kikuchi, A., Fiesel, F.C., Sasaki, T., Aoki, M., Itoyama, Y., and Takeda, A. (2012). Suppression of dynamin GTPase decreases alpha-synuclein uptake by neuronal and oligodendroglial cells: a potent therapeutic target for synucleinopathy. Mol. Neurodegener. *7*, 38.

Lee, Y., Morrison, B.M., Li, Y., Lengacher, S., Farah, M.H., Hoffman, P.N., Liu, Y., Tsingalia, A., Jin, L., Zhang, P.W., et al. (2012). Oligodendroglia metabolically support axons and contribute to neurodegeneration. Nature *487*, 443–448.

Levine, J.M., Reynolds, R., and Fawcett, J.W. (2001). The oligodendrocyte precursor cell in health and disease. Trends Neurosci. *24*, 39–47.

Maki, T., Takahashi, Y., Miyamoto, N., Liang, A.C., Ihara, M., Lo, E.H., and Arai, K. (2015). Adrenomedullin promotes differentiation of oligodendrocyte precursor cells into myelin-basic-protein expressing oligodendrocytes under pathological conditions in vitro. Stem Cell Res. *15*, 68–74.

Masuda-Suzukake, M., Nonaka, T., Hosokawa, M., Oikawa, T., Arai, T., Akiyama, H., Mann, D.M., and Hasegawa, M. (2013). Prion-like spreading of pathological alpha-synuclein in brain. Brain *136*, 1128–1138.

May, V.E., Ettle, B., Poehler, A.M., Nuber, S., Ubhi, K., Rockenstein, E., Winner, B., Wegner, M., Masliah, E., and Winkler, J. (2014). alpha-Synuclein impairs oligodendrocyte progenitor maturation in multiple system atrophy. Neurobiol. Aging *35*, 2357–2368.

Miller, D.W., Johnson, J.M., Solano, S.M., Hollingsworth, Z.R., Standaert, D.G., and Young, A.B. (2005). Absence of alpha-synuclein mRNA expression in normal and multiple system atrophy oligodendroglia. J. Neural Transm. (Vienna) *112*, 1613–1624.

Mutka, A.L., Haapanen, A., Kakela, R., Lindfors, M., Wright, A.K., Inkinen, T., Hermansson, M., Rokka, A., Corthals, G., Jauhiainen, M., et al. (2010). Murine cathepsin D deficiency is associated with dysmyelination/myelin disruption and accumulation of cholesteryl esters in the brain. J. Neurochem. *112*, 193–203.

Richter-Landsberg, C., Gorath, M., Trojanowski, J.Q., and Lee, V.M. (2000). alpha-synuclein is developmentally expressed in cultured rat brain oligodendrocytes. J. Neurosci. Res. *62*, 9–14.

Schwarz, L., Goldbaum, O., Bergmann, M., Probst-Cousin, S., and Richter-Landsberg, C. (2012). Involvement of macroautophagy in multiple system atrophy and protein aggregate formation in oligodendrocytes. J. Mol. Neurosci. *47*, 256–266.

Shults, C.W., Rockenstein, E., Crews, L., Adame, A., Mante, M., Larrea, G., Hashimoto, M., Song, D., Iwatsubo, T., Tsuboi, K., and Masliah, E. (2005). Neurological and neurodegenerative alterations in a transgenic mouse model expressing human alpha-synuclein under oligodendrocyte promoter: implications for multiple system atrophy. J. Neurosci. *25*, 10689–10699.

Volpicelli-Daley, L.A., Luk, K.C., Patel, T.P., Tanik, S.A., Riddle, D.M., Stieber, A., Meaney, D.F., Trojanowski, J.Q., and Lee, V.M. (2011). Exogenous alpha-synuclein fibrils induce Lewy body pathology leading to synaptic dysfunction and neuron death. Neuron *72*, 57–71.

Wenning, G.K., Stefanova, N., Jellinger, K.A., Poewe, W., and Schlossmacher, M.G. (2008). Multiple system atrophy: a primary oligodendrogliopathy. Ann. Neurol. *64*, 239–246.

Wilkins, A., Majed, H., Layfield, R., Compston, A., and Chandran, S. (2003). Oligodendrocytes promote neuronal survival and axonal length by distinct intracellular mechanisms: a novel role for oligodendrocyte-derived glial cell line-derived neurotrophic factor. J. Neurosci. *23*, 4967–4974.

Stem Cell Reports, Volume *10*

Supplemental Information

Pathological Endogenous α-Synuclein Accumulation in Oligodendrocyte Precursor Cells Potentially Induces Inclusions in Multiple System Atrophy

Seiji Kaji, Takakuni Maki, Hisanori Kinoshita, Norihito Uemura, Takashi Ayaki, Yasuhiro Kawamoto, Takahiro Furuta, Makoto Urushitani, Masato Hasegawa, Yusuke Kinoshita, Yuichi Ono, Xiaobo Mao, Tran H. Quach, Kazuhiro Iwai, Valina L. Dawson, Ted M. Dawson, and Ryosuke Takahashi

Supplemental Information: Extended Experimental Procedures

Pathological Endogenous α-Synuclein Accumulation in Oligodendrocyte Precursor Cells Potentially Induces Inclusions in Multiple System Atrophy

Authors: Seiji Kaji, MD, Takakuni Maki, MD, PhD, Hisanori Kinoshita, MD, Norihito Uemura, MD, PhD, Takashi Ayaki, MD, PhD, Yasuhiro Kawamoto, MD, PhD, Takahiro Furuta, PhD, Makoto Urushitani, MD, PhD, Masato Hasegawa, PhD, Yusuke Kinoshita, Yuichi Ono, PhD, Xiaobo Mao, PhD, Tran H. Quach, Kazuhiro Iwai, MD, PhD, Valina L. Dawson, PhD, Ted M. Dawson, MD, PhD, Ryosuke Takahashi, MD, PhD

Inventory of Supplemental Information

Supplemental Experimental Procedures:

Histopathological Analysis of MSA Patients

For histopathological analysis, formalin-fixed, paraffin-embedded 6-μm-thick sections from the pons of MSA patients were deparaffinized and immunostained. We applied primary antibodies for α-synuclein (α-syn) (1:200, BD Biosciences, 610787) and NG2 (1:200, Merck Millipore, AB5320) and incubated overnight at 4°C. Subsequently to incubation with secondary antibodies (1:200, Alexa Fluor 594 and 647, A21207, A31571) for 1 hour at room temperature, sections were covered with VECTASHIELD mounting medium (Vector Laboratories) with DAPI. For Thioflavin S assessment, sections were incubated with 20 μM Thioflavin S (Sigma Aldrich) in distilled water for 20 min at room temperature before mounting. Images were obtained using a confocal microscopy as described below. Procedures involving the use of human materials were performed in accordance with ethical guidelines set by Kyoto University.

Primary Cell Cultures

Primary oligodendrocyte lineage cell and other glial cell culture

OPCs were prepared as previously described (Maki et al., 2015). Briefly, cerebral cortices from 1- to 2-day-old Sprague Dawley rats (Shimizu Laboratory Supplies Co., Ltd) were dissected, minced, and digested. Dissociated cells were plated in poly-D-lysine-coated 75 cm^2 flasks, and maintained in Dulbecco's Modified Eagle's Medium (DMEM) containing 20% heat-inactivated fetal bovine serum and 1% penicillin/streptomycin. After the cells were confluent (~10 days), the flasks were shaken for 1 hour on an orbital shaker (220 rpm) at 37°C to remove microglia. The flasks were then changed to new medium and shaken overnight (~20 hours). The medium was collected and plated on non-coated tissue culture dishes for 1 hour at 37°C to eliminate contaminating astrocytes and microglia. The non-adherent cells (OPCs) were collected and replated at a density of 20,000 cells/cm^2 in Neurobasal (NB) medium containing 2 mM glutamine, 1% penicillin/streptomycin, 10 ng/ml PDGF-AA, 10 ng/ml FGF-2 and 2% B27 supplement onto poly-DL-ornithine-coated plates. Four to 6 days after plating, the OPCs were used for the experiments. To differentiate OPCs to mature oligodendrocytes, the culture medium was switched to DMEM containing 1% penicillin/streptomycin, 10 ng/ml CNTF, 15 nM T3 and 2% B27 supplement. Seven days after switching medium, the mature oligodendrocytes were used for the experiments. To obtain astrocytes, non-astrocytic cells were detached from the flasks with mixed glial cells by shaking and removing the medium. Then, astrocytes were dissociated by tripsinization and subsequently replated at a density of 200,000 cells/cm^2.

Primary neuronal cell culture

Cortical neuronal cultures were prepared from 17-day-old Sprague Dawley rat embryos (Shimizu Laboratory Supplies Co., Ltd) using methods described earlier (Maki et al., 2014). Briefly, cortices were dissected and dissociated. Cells were plated on dishes coated with poly-D-lysine in DMEM containing

5% fetal bovine serum and 1% penicillin/streptomycin at a density of 200,000 cells/cm^2. At 24-hour after seeding, the medium was changed to NB medium containing 0.5 mM glutamine, 1% penicillin/streptomycin and 2% B27 supplement. Cultured neurons were used for experiments 14 days after seeding.

Preparation of Recombinant Human α-Syn PFFs

Purification was conducted in accordance with previously established method (Masuda-Suzukake et al., 2013). Human wild-type α-syn cDNA was cloned into the bacterial expression vector pRK172. Transformations and selection were performed using E. coli BL-21(DE3) competent cells (BioDynamics) and ampicillin (100 μg/ml) in Luria-Bertani media. Following overnight incubation of transformed cells in Luria-Bertani media containing ampicillin (100 μg/ml) at 37 °C, the culture was incubated for another 5 hours after 300-fold dilution and then induced with 1mM isopropyl-β-D-thiogalactopyranoside for 5 hours at 37 °C. Bacterial pellets were resuspended in high-salt buffer (1M Tris-HCl, pH 7.5, 1 mM EDTA), heated to 100 °C for 5 min, and centrifuged at 15,000 rpm for 15 min. The supernatants were subjected to chromatography on a Q-Sepharose fast-flow column (GE healthcare) with a gradient of 0 to 0.5 M NaCl in Tris buffer. The proteins were dialyzed overnight against 50 mM Tris-HCl, 150 mM KCl, pH 7.5 and centrifuged at 55,000 rpm at 4°C for 20 min. The supernatants were filtered with 0.2 μm syringe filters (Life Sciences) and diluted in media for experimental use as monomeric α-syn. For PFFs formation, proteins were incubated with constant agitation at 37°C for 3-7 days. α-Syn PFFs were diluted in PBS at 1 μM or 3 μM, sonicated several times (30-60 seconds in total), filtered with 0.2 μm syringe filters (Life Sciences), and diluted in media. For observation with confocal and immunoelectron microscopy, 3 μM and 1 μM α-syn PFFs or monomer were prepared, respectively. The fractions were assayed for the presence of the α-syn proteins by SDS-polyacrylamide gel electrophoresis (PAGE) followed by Coomassie Blue R-250 staining. Protein concentration was determined using the bicinchoninic acid protein assay (Thermo Fisher) and bovine serum albumin as a standard.

Incubation of OPCs with Autophagy-Modifying Drugs

To assess how altered autophagic states affect the endogenous α-syn expression and autophagic markers in OPCs, we incubated OPCs for 24 hours with 10 μM chloroquine (Enzo Life Science), a lysosomal inhibitor, or 500 nM rapamycin (Enzo Life Science), an autophagy inducer.

Differentiation of OPCs Pre-incubated with α-Syn PFFs

1 μM or 3 μM α-syn PFFs were added to OPCs culture when its confluency reaches 60%. Subsequently to 24-hour incubation with α-syn PFFs, cells were washed twice with fresh medium not containing α-syn PFFs. Medium was switched to DMEM containing 1% penicillin/streptomycin, 10 ng/ml CNTF, 15 nM T3 and 2% B27 supplement. After 7 days of incubation, the mature oligodendrocytes were used for the

experiments.

Incubation of Primary Cortical Neurons with Conditioned Medium from OLGs

Primary cortical neuron culture was incubated for 72 hours either 1) with conditioned medium from normal OLGs, 2) with conditioned medium from OLGs differentiated from OPCs preincubated with α-syn PFFs (3 μM), or 3) with neuron medium incubated for 24 hours in no cell plate (serves as control). Conditioned medium was prepared from neuron medium (NB medium containing 0.5 mM glutamine, 1% penicillin /streptomycin and 2% B27 supplement) which were incubated for 24 hours with mature OLGs differentiated from OPCs with or without α-syn PFFs preincubation (as illustrated in Fig. 4A).

Time-Lapse Imaging

Time-lapse imaging was performed with BZ-X710 (Keyence) equipped with an incubator (37°C and 5% CO2) by acquiring images at defined positions every 10 minutes. Images were converted to AVI files.

Cathepsin D activity Assay

The enzymatic activity of cathepsin D in OPCs was measured by cathepsin D assay kit (AnaSpec) according to the manufacturer's instructions. Cathepsin activity was determined by kinetic analysis, which calculates the initial reaction velocity in relative fluorescence units (RFU) per minute. RFU change during the first 5 minutes of the reaction was used for the calculation.

Cytotoxicity and Cell Survival Assay with Media LDH and WST Assay

Cytotoxicity was assessed by media LDH assay kit (Cytotoxicity LDH Assay Kit-WST, Dojindo). LDH is rapidly released into the cell-culture supernatants when the plasma membrane is damaged. 100 μl of the supernatants is incubated with the same amount of substrate mixture from the kit for 30 min. Then the absorbance of the culture medium was measured with a microplate reader at a test wavelength of 490 nm.
Cell proliferation/survival was assessed by WST reduction assay kit (Cell Counting Kit-8, Dojindo). WST assay is a sensitive colorimetric method to detect cell viability. The cells were incubated with 10% WST solution for 1 hour at 37°C. The absorbance of the culture medium was measured at a wavelength of 450 nm and a reference wavelength of 630 nm.

Immunostainings with Confocal Microscopy

After washing the cells twice with PBS, the cells were fixed with 4% PFA for 15 min. After washing twice with PBS, incubation with PBS/0.1%Tween (10 min) and blocking with 3%BSA/PBS (1 hour at room temperature), the cells were incubated with primary antibodies against PDGFRα (1:200, R&D systems, AF1062), MBP (1:200, MBL, PD004 or 1:200, Thermo Fisher Scientific, MA1-10837), α-syn (recognizes human and rat) (1:200, BD Biosciences, 610787), rat α-syn (1:200, CST, 4179S), human

α-syn (1:200, Thermo Fisher Scientific, 180215), TPPP/p25α (1:200, Abcam, ab92305), p62 (200:1, MBL, PM045), Beclin-1 (200:1, Santa Cruz, sc-10086), LC3 (300:1, MBL, PM036), phosphorylated α-syn (1:200, Abcam, ab51253), MAP2 (300:1, Sigma Aldrich, M1406) and NeuN (300:1, Merck Millipore, ABN78) at 4°C overnight. For the validation of endogenous α-syn expression in OPCs, we used Mouse-IgG (200:1, Vector Laboratories, BA-2000) as a primary antibody for negative control. Subsequently, after washing with PBS, they were incubated with secondary antibodies (1:200, Alexa Fluor 488, 594 and 647, A21202, A21203, A31571, A21206, A21207, A31573, A11055, A11058, A21447) for 1 hour at room temperature. After washing with PBS, the cells were covered with VECTASHIELD mounting medium (Vector Laboratories) with DAPI. The cells were observed by Olympus Fluoview FV1000 confocal microscope (Olympus). As for Thioflavin S staining, cells were incubated with 20 μM Thioflavin S (Sigma Aldrich) in distilled water for 20 min at room temperature before mounting. Image analysis and 3D surface reconstruction were performed by FV10-ASW software (Olympus). Sections were imaged at 0.124 μm/pixel resolution in xy dimension and 0.4 μm in z dimension. Regarding the use of the LysoTracker (Life technologies) probes, cells were incubated with probe-containing medium (50 nM) for 30 minutes, before the wash with PBS and fixation. The following immunostaining was conducted as described above.

Immunoelectron Microscopy

Immunoelectron microscopy using ultrathin cryosections was performed as described. Briefly, cells were washed with PBS twice, immersed in 4% PFA with 0.1% glutaraldehyde at 4°C for 2 hours. Following 60 min pre-treatment with 3% BSA in PBS used for blocking agents containing 0.1 % Photo-Flo (EMS), the samples were incubated overnight at 4°C with mouse anti-α-syn antibody (1:200, BD Biosciences, 610787). They were then incubated with Nanogold goat anti-mouse IgG conjugates (1:100, Nanoprobes, 2002) overnight at 4°C. Immunostained sections were fixed with 1% glutaraldehyde in 0.1M PB. To better visualize the particles, the samples were reacted with Silver Enhancement Kit solutions (Nanoprobes) The sections were then washed with 0.1 M PB, placed for 40 min in 0.1 M PB containing 1% osmium tetroxide, dehydrated, and embedded in epoxy resin (Luveak 812; Nacalai Tesque, Kyoto, Japan). After polymerization of the resin, each tissue sample was cut into 70-nm-thick ultrathin sections with a diamond knife on an ultramicrotome (Leica EM UC6 , Heiderberg, Germany), and mounted on coated copper grids (Stork Veco, Eerbeek, The Netherlands). The sections were finally examined with an electron microscope (H-7650; Hitachi, Tokyo, Japan) at 80 kV (Kameda et al., 2012).

Immunoblot Analysis

Cells were rinsed twice with PBS and collected into sample buffer containing 50% Tris-Glycine SDS buffer (Novex), 45% RIPA buffer (20 mM HEPES-KOH pH 7.4, 150 mM NaCl, 2 mM EDTA, 1% Nonidet-P40, 1% sodium deoxycholate), 5% 2-mercaptomethanol (Nacalai tesque),.1% phosphatase

inhibitor (Nacalai tesque) and 1% protease inhibitor (Nacalai tesque). Subsequently, samples were heated at 95°C for 5 min, and each sample was loaded onto 5–20% or 15 % polyacrylamide gel (Wako). After electrophoresis and transferring onto a PVDF membrane (Merck Millipore), the membranes were fixed with 4%PFA for 30 min and blocked in Tris buffered saline with 0.1% Tween 20 (TBS-T) containing 5% nonfat dry milk for 60 min at room temperature. Membranes were then incubated overnight at 4°C with primary antibodies for α-syn (recognizes human and rat) (1:1000, BD Biosciences, 610787), rat α-syn (1:1000, CST, 4179S), human α-syn (1:500, Thermo Fisher Scientific, 180215), PDGFRα (1:500, R&D systems, AF1062), MBP (1:1000, Thermo Fisher Scientific, MA1-10837), TPPP/p25α (1:500, Abcam, ab92305) GFAP (1:5000, Thermo Fisher Scientific, 13-0300), NeuN (3000:1, Merck Millipore, ABN78), GAPDH (500:1, Santa Cruz Biotechnology, sc-25778), HSP90α (1:5000, Abcam, ab133491), sodium potassium ATPase (1:5000, Abcam, ab76020), p62 (500:1, MBL, PM045), LC3 (500:1, MBL, PM036), Beclin-1 (500:1, Santa Cruz, sc-48341), cathepsin D (500:1, Santa Cruz Biotechnology, sc-6486), lysine-48-specific ubiquitin (Merck Millipore, 1000:1, 05-1307) or anti-β-actin antibody (1:10000, Sigma Aldrich, A5441), followed by 60 min incubation with secondary goat or donkey anti-IgG HRP antibodies (Santa Cruz Biotechnology, NA9310V, NA9340V, NB7115, NB7357) and visualization by enhanced chemiluminescence (Nacalai tesque). Assessment of Triton-insoluble SDS-soluble fractions was conducted as previously described (Uemura et al., 2015). Cells were homogenized in lysis buffer containing 1% Triton X-100 (150 mM NaCl, 50 mM Tris-HCl, 1% Triton X-100, pH 7.5) and centrifuged at 55,000 rpm at 4°C for 30 min. The supernatants were used for Triton soluble fractions. For SDS-soluble fractions, the pellet was rinsed with the lysis buffer, centrifuged again at 55,000 rpm at 4°C for 30 min followed by removal of the supernatant. Subsequently, the pellet was sonicated in SDS buffer (50 mM Tris-HCl, 2% SDS, pH 7.4) followed by centrifugation at 55,000 rpm at 4°C for 30 min. The supernatant was boiled in sample buffer (1% SDS, 12.5% glycerol, 0.005% bromophenol blue, 2.5% 2-mercaptoethanol, 25 mM Tris-HCl, pH 6.8). Samples containing 20 μg of proteins were loaded onto each lane of 10 % Bis-Tris gels (Novex) for both fractions. The following procedure was performed as mentioned above. Each band was quantified with image J or ImageQuant software (GE healthcare) (Schneider et al., 2012).

Subcellular Fractionation

Trident Membrane Protein Extraction Kit (GeneTex) was used for subcellular fractionation. Extraction of cytosolic and plasma membrane fraction was conducted according to the manufacturer's instructions.

RNA-seq Analysis in OPCs

Library construction and sequencing

RNA-Seq library and sequencing: Agilent SureSelect Strand Specific RNA prep kit (Cat# G9691A) was used with 200ng of total RNA for the construction of cDNA libraries according to the manufacturer's

protocol. All cDNA libraries were sequenced using an Illumina Miseq, producing 76×2 bp paired-end reads with multiplexing.

Bioinformatics analysis

All raw sequencing reads were trimmed using Trimmomatic software (Bolger et al., 2014). Bases and QC assessment of sequencing were generated by FastQC. QC-passed reads were aligned to the Ensembl Rnor 6.0.84 reference genome using Star v2.5.0c (Dobin et al., 2013). The abundance of transcripts was then estimated using an Expectation-Maximization algorithm implemented in the software package Cufflnk v2.2.1 [http://cole-trapnell-lab.github.io/cufflinks/]. Drawing heatmap of the RNA-seq data was performed using R software and the ggplot2 package

Quantitative Real-time PCR

RNA was extracted from cells with RLT lysis buffer (QIAGEN) according to the manufacturer's instructions. RNA concentration was measured by NanoDrop 1000 spectrometer (Thermo Scientific). cDNA was generated with reverse transcription using the PrimeScript RT reagent kit (TaKaRa). The amount of cDNA was quantified with real-time PCR using LightCycler 480 SYBR Green I Master (Roche) and Roche LightCycler 480. The primer sets used in this study is listed in Table S1, thereafter.

Statistical Analysis

All quantitative data were analyzed using Prism 5.0 (Graphpad). Statistical significance was evaluated using a paired t-test or a one-way ANOVA followed by Tukey's honestly significant difference test for multiple comparisons. Data are expressed as mean ± S.D. A p-value of <0.05 was considered statistically significant.

Supplemental Results:

α-Syn PFF Receptor Membrane Proteins in Oligodendrocyte Lineage Cells

A recent report using primary neurons suggested that lymphocyte-activation gene 3 (LAG3) selectively binds to α-syn PFFs and mediates endocytosis as well as cell-to-cell transmission (Mao et al., 2016). Unexpectedly, our RNA-seq analysis suggested that the basal gene expression levels of *Lag3* in OPCs were very low (Fig. S3K). The LAG3 protein expression in OPCs was also relatively low in immunoblot analysis (data not shown), and the pathological function of LAG3 in oligodendrocyte lineage cells remains unclear.

Supplemental Discussion:

Our studies demonstrated the predominance of α-syn internalization and susceptibility against seeding in OPCs, and indicated the possibility that OPCs are more relevant to the propagation of misfolded α-syn than OLGs. As is previously demonstrated with neurons, internalization of exogenous α-syn in oligodendroglial cells is presumably mediated by endocytosis (Konno et al., 2012; Mao et al., 2016). In fact, according to our RNA-seq analysis, the gene expressions of endocytic proteins such as Rab5a, Rab7a and Rab7b in OPCs seemed to increase after α-syn PFFs application (Fig. S3K). Nevertheless, the gene expressions of possible candidate receptors for misfolded α-syn, such as clathrin and LAG3, remained basically unchanged. A variety of endocytic pathways need to be scrutinized to unravel the seeding mechanisms lying behind our *in vitro* study results. In our study, however, the involvement of endocytic pathway was difficult to confirm, due to the limited tolerability of primary OPCs against the cytotoxicity of dynamin or clathrin inhibitor. In terms of *in vivo* propagation of misfolded α-syn, injection of α-syn PFFs into brains usually leads to α-syn aggregate formation exclusively in neurons. As far as OPCs are concerned, sparse basal expression levels of an α-syn PFF receptor protein, LAG3, may be consistent with these *in vivo* observations.

Supplemental References

Bolger AM, Lohse M, Usadel B (2014) Trimmomatic: a flexible trimmer for Illumina sequence data. Bioinformatics (Oxford, England) 30:2114-2120.

Dobin A, Davis CA, Schlesinger F, Drenkow J, Zaleski C, Jha S, Batut P, Chaisson M, Gingeras TR (2013) STAR: ultrafast universal RNA-seq aligner. Bioinformatics (Oxford, England) 29:15-21.

Kameda H, Hioki H, Tanaka YH, Tanaka T, Sohn J, Sonomura T, Furuta T, Fujiyama F, Kaneko T (2012) Parvalbumin-producing cortical interneurons receive inhibitory inputs on proximal portions and cortical excitatory inputs on distal dendrites. The European journal of neuroscience 35:838-854.

Konno M, Hasegawa T, Baba T, Miura E, Sugeno N, Kikuchi A, Fiesel FC, Sasaki T, Aoki M, Itoyama Y, Takeda A (2012) Suppression of dynamin GTPase decreases alpha-synuclein uptake by neuronal and oligodendroglial cells: a potent therapeutic target for synucleinopathy. Molecular neurodegeneration 7:38.

Maki T, Takahashi Y, Miyamoto N, Liang AC, Ihara M, Lo EH, Arai K (2015) Adrenomedullin promotes differentiation of oligodendrocyte precursor cells into myelin-basic-protein expressing oligodendrocytes under pathological conditions in vitro. Stem cell research 15:68-74.

Maki T, Okamoto Y, Carare RO, Hase Y, Hattori Y, Hawkes CA, Saito S, Yamamoto Y, Terasaki Y, Ishibashi-Ueda H, Taguchi A, Takahashi R, Miyakawa T, Kalaria RN, Lo EH, Arai K, Ihara M (2014) Phosphodiesterase III inhibitor promotes drainage of cerebrovascular beta-amyloid. Annals of clinical and translational neurology 1:519-533.

Mao X et al. (2016) Pathological alpha-synuclein transmission initiated by binding lymphocyte-activation gene 3. Science (New York, NY) 353.

Masuda-Suzukake M, Nonaka T, Hosokawa M, Oikawa T, Arai T, Akiyama H, Mann DM, Hasegawa M (2013) Prion-like spreading of pathological alpha-synuclein in brain. Brain : a journal of neurology 136:1128-1138.

Schneider CA, Rasband WS, Eliceiri KW (2012) NIH Image to ImageJ: 25 years of image analysis. Nature methods 9:671-675.

Uemura N, Koike M, Ansai S, Kinoshita M, Ishikawa-Fujiwara T, Matsui H, Naruse K, Sakamoto N, Uchiyama Y, Todo T, Takeda S, Yamakado H, Takahashi R (2015) Viable neuronopathic Gaucher disease model in Medaka (Oryzias latipes) displays axonal accumulation of alpha-synuclein. PLoS genetics 11:e1005065.

Table S1 Table of Primers Used in This Study

Gene name	Abbreviations	Direction	Sequences
α-synulcien	*Snca*	F	CAACAGTGGCTGAGAAGACC
		R	GAAGGCATTTCATAAGCCTC
Platelet-derived growth factor receptor, α	*Pdgfra*	F	CTAATTCACATTCGGGAAGGTTG
		R	GGACGATGGGCGACTAGAC
Oligodendrocyte transcription factor 2	*Olig2*	F	GACGACATTATGGGCTTTGATGG
		R	GTTTCTGCCTGAACAGTCCAC
Neural/Glial antigen 2	*Cspg4*	F	ATGCCCACTGTAGCCAAAAG
		R	GTGTCACCAGCTAGGCCATT
Nestin	*Nes*	F	CGCCGCTACTTCTTTTCAAC
		R	GCAGCTGGTTTTGCTCTTCT
Myelin basic protein	*Mbp*	F	ACACACAAGAACTACCCACTACGG
		R	AGCTAAATCTGCTGAGGGACAG
Myelin associated glycoprotein	*Mag*	F	ATTCCGAATCTCTGGAGCAC
		R	ACTCAGCCAGCTCCTCTGTC
Glial fibrillary acidic protein	*Gfap*	F	AGAAAACCGCATCACCATTC
		R	GCACACCTCACATCACATCC
Neuron-specific class III β-tublin (Tuj-1)	*Tubb3*	F	ACTTTATCTTCGGTCAGAGTG
		R	CTCACGACATCCAGGACTGA
Monocarboxylate transporter (MCT-1)	*Slc16a1*	F	CTTGTGGCGTGATCCT
		R	GTTTCGGATGTCTCGGG
Brain-derived neurotrophic factor	*Bdnf*	F	ATAGGAGACCCTCCGCAACT
		R	CTGCCATGCATGAAACACTT
Glial cell line-derived neurotrophic factor	*Gdnf*	F	GCGGTTCCTGTGAAGCGGCCGA
		R	TAGATACATCCACACCGTTTAGCGG
Insulin like growth factor 1	*Igf-1*	F	CAGTTCGTGTGTGGACCAAG
		R	GTCTTGGGCATGTCAGTGTG
Glyceraldehyde-3-phosphate dehydrogenase	*Gapdh*	F	TCCCGCTAACATCAAATGGG
		R	CCATCCACAGTCTTCTGAGT

F; forward, R; reverse

Supplemental Figure S1

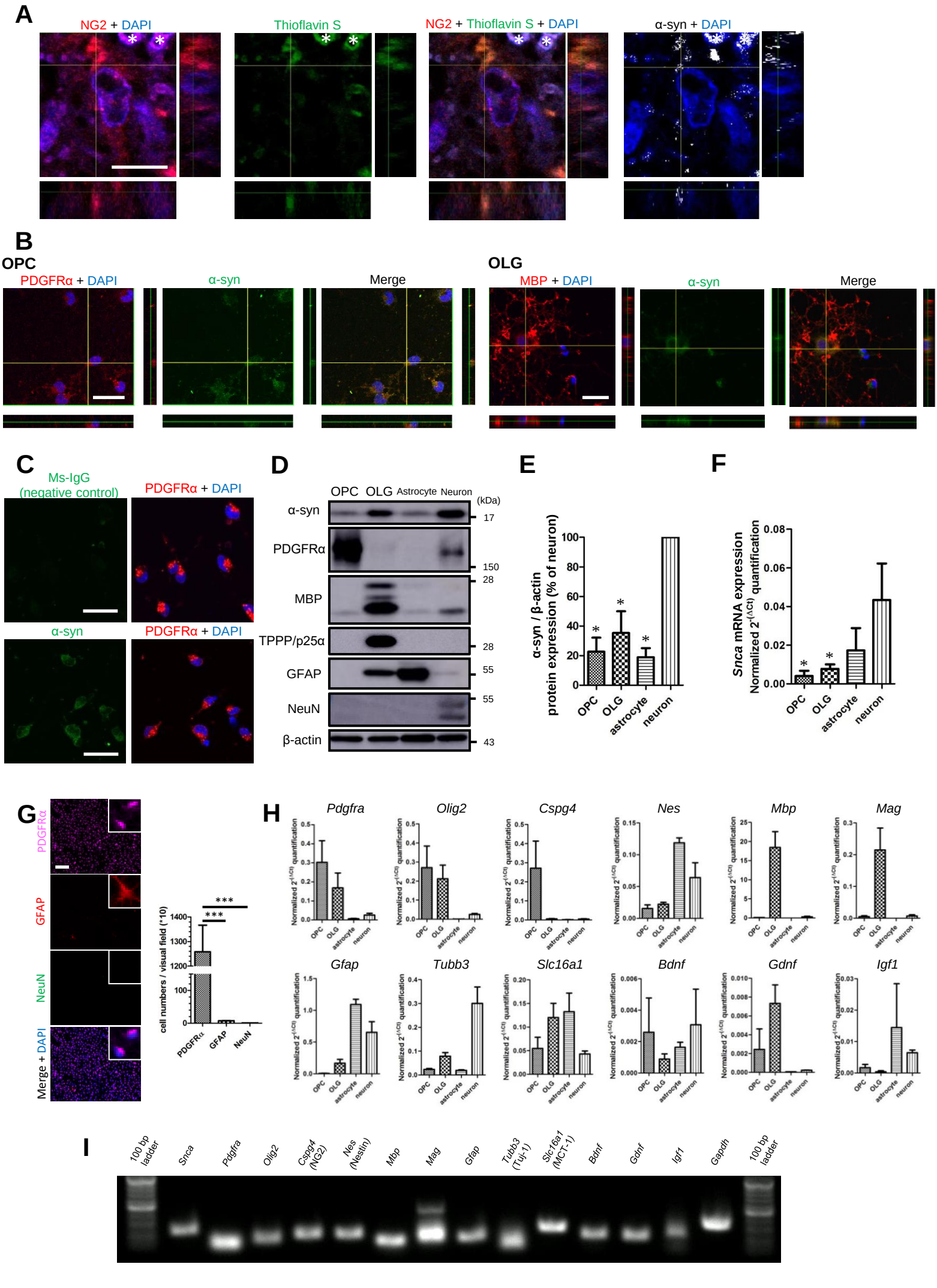

Figure S1 Identification of α-Syn Accumulation in OPCs of an MSA Brain, and *In Vitro*α-Syn Expression in Primary Oligodendrocyte Lineage Cell Culture

MSA Brain

(A) The $NG2^+$ OPC contains Thioflavin S-immunopositive aggregates, which are immunoreactive to α-syn in the pons of an MSA patient. The images were acquired by confocal microscopy. The white asterisks indicate erythrocytes. The scale bar represents 10μm.

Primary Oligodendrocyte Lineage Cells

(B) Confocal microscopy reveals α-syn immunoreactivity in both the cytoplasm of OPCs and OLGs. The scale bars represent 20 μm.

(C) The α-syn immunoreactivity in OPCs is guaranteed by validating the difference between immunostaining results with mouse-IgG and anti-α-syn antibody (mouse-derived). The scale bars represent 20 μm.

(D) Immunoblot analysis with an anti-α-syn antibody and antibodies against each cell-type marker illustrates α-syn expression in oligodendrocyte lineage cells as well as sufficiently high cell purity of each primary culture.

(E) Quantification of α-syn expression in each cell type by immunoblot analysis verifies the appreciable levels of α-syn protein expressions in oligodendrocyte lineage cells. Relative α-syn expressions in glial cells with respect to that in neurons are illustrated. Mean±SEM; n=3, respectively; independent cultures; one-way ANOVA, *$p<0.05$ (compared with neuronal expression).

(F) Quantitative real-time PCR analysis confirms the *Snca* mRNA expression in each cell-type culture. Mean±SEM; n=6 for OPCs and OLGs, n=3 for astrocytes and neurons; independent cultures; one-way ANOVA, *$p<0.05$ (compared with neuronal expression).

(G) The purity of OPC culture is validated by immunostaining using antibodies against PDGFRα, GFAP, and NeuN. The scale bar represents 100μm. Cell numbers per each ×175 magnified visual field were quantified. Mean±SEM; n=3, respectively; one-way ANOVA, ***$p<0.001$.

(H) Quantitative real-time PCR shows each cell marker transcript and neuromodulating factors. Mean±SEM; n=6 for OPCs and OLGs, n=3 for astrocytes and neurons, independent cultures.

(I) Validation of primers used for quantitative real-time PCR is shown.

Supplemental Figure S2

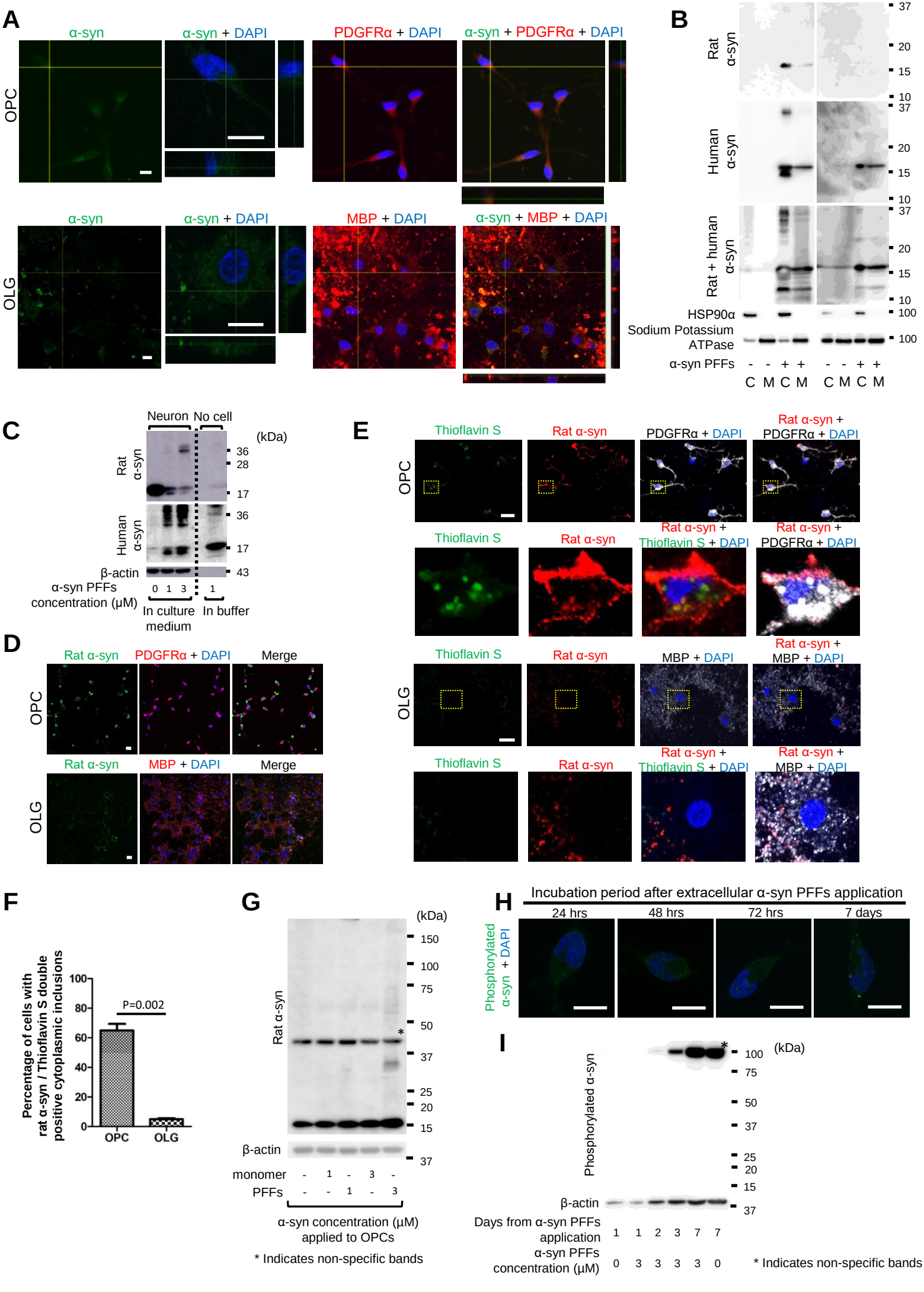

Figure S2 Characterization of Cytoplasmic Inclusions in Oligodendroglial Cells; Extracellular α-Syn PFFs Trigger the Aggregation of Endogenous Rat α-Syn Predominantly in OPCs

(A) Confocal microscopy of OPCs and OLGs incubated with recombinant human α-syn monomer (3 μM) shows no evident cytoplasmic α-syn accumulation. The primary antibody used for the immunostaining recognizes both exogenous human and endogenous rat α-syn. Each scale bar represents 10 μm.

(B) Subcellular fractionation of OPCs and OLGs shows cytosolic accumulation of endogenous rat and exogenous human α-syn in OPCs in response to 24-hour incubation with recombinant human α-syn pre-formed fibrils (α-syn PFFs). Dimerization of endogenous rat α-syn is also observed in the cytosolic fraction in OPCs. C = cytoplasmic fraction; M = plasma membrane fraction.

(C) Immunoblot analysis of primary rat neurons verifies the specific detection of endogenous α-syn by the rat-specific anti-α-syn antibody. The far right lane represents 1 μM of α-syn PFFs without cell lysates, which is recognized only with human-specific anti-α-syn antibody guaranteeing the specificity of each antibody. Endogenous rat α-syn in neurons is also multimerized by 24-hour incubation with α-syn PFFs.

(D) Enhanced immunoreactivity of endogenous rat α-syn is observed predominantly in α-syn PFFs-treated OPCs labeled with PDGFRα. OLGs are labeled with MBP. The scale bar represents 20 μm.

(E) Magnified views of α-syn PFFs-treated oligodendroglial cells by confocal microscopy reveal Thioflavin S-positive inclusions extensively observed in OPCs, but not in OLGs. Each magnified oligodendroglial cell corresponds to the cells surrounded by the dotted yellow lines. Each scale bar represents 20 μm.

(F) Percentages of cells containing endogenous rat α-syn/Thioflavin S double-positive inclusions are quantified in OPC and OLG culture. The intracellular localization of each inclusion is confirmed by each cell marker, PDGFRα or MBP. Mean±SEM; n=3, respectively; independent cultures; one-way ANOVA.

(G) Immunoblot analysis of OPCs incubated with monomeric or fibrillar recombinant human α-syn shows different response of endogenous rat α-syn expressions. Multimerization is not observed with the application of monomeric α-syn.

(H) (I) Phosphorylated α-syn is not detected within a timeframe of 7 days after α-syn PFFs (3 μM) application to OPCs. Each scale bar represents 10 μm.

Supplemental Figure S3

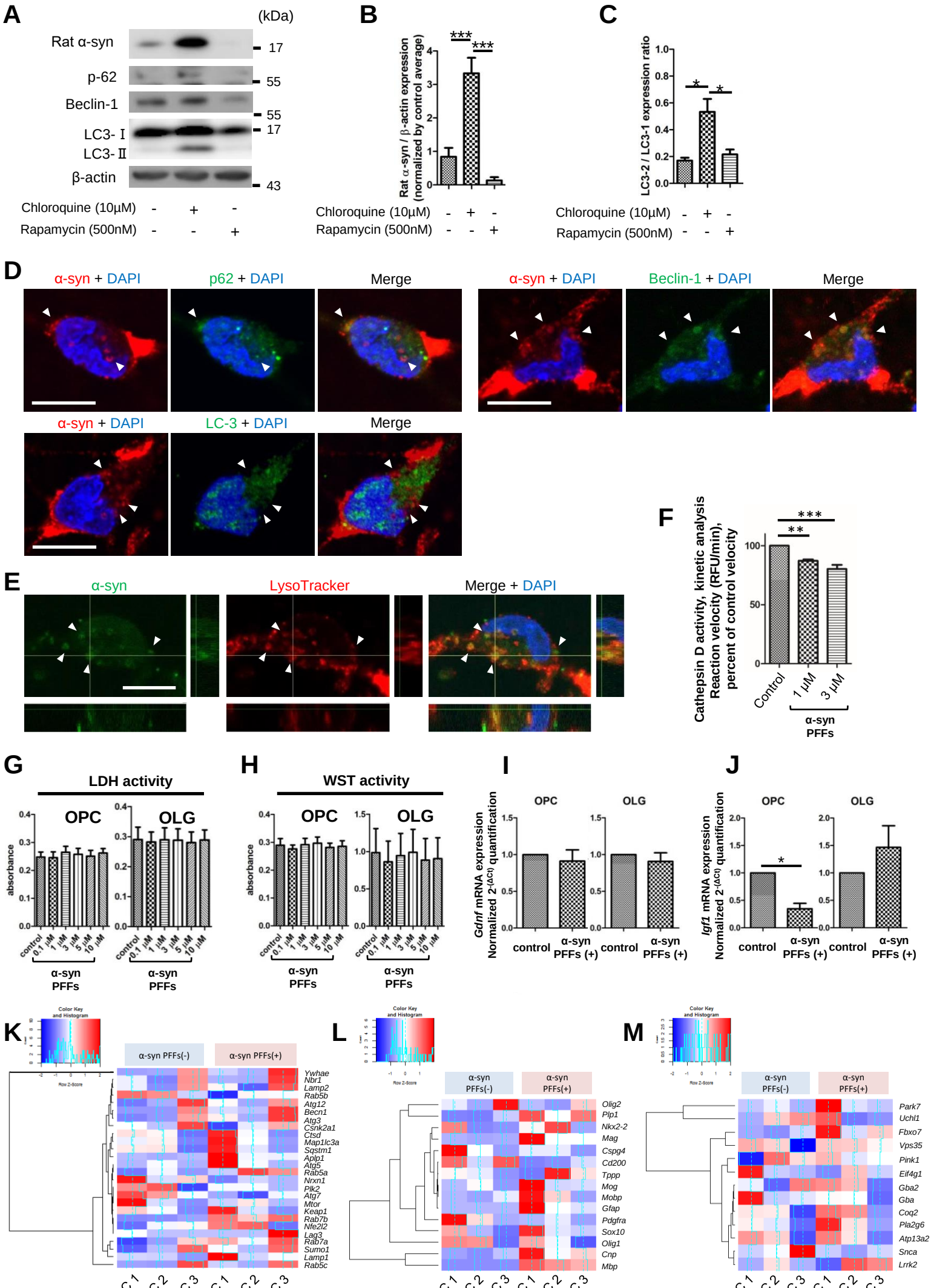

Figure S3 Autophagic Response and Functional Influence Induced by α-Syn PFFs Application to OPCs

(A) Immunoblot analysis of OPCs after 24-hour incubation with chloroquine (10 μM) or rapamycin (500 nM). Chloroquine induced increased expressions of endogenous rat α-syn, p-62, Beclin-1, and LC3-II, while rapamycin induced suppression of these protein expressions.

(B) (C) Quantification of (B) the endogenous rat α-syn expression and (C) the LC3-II / LC3-I ratio is displayed. Mean±SEM; n=4, respectively; independent cultures; one-way ANOVA. *$p<0.05$, ***$p<0.001$.

(D) Immunoblot analysis of α-syn PFFs-treated OPCs labeled with antibodies against autophagic markers, p62, Beclin-1, and LC3, shows the interaction of α-syn with these autophagic markers (as indicated by white arrowheads). Each scale bar represents 10 μm.

(E) Lysosomal localization of α-syn is revealed by LysoTracker (as indicated by white arrowheads) 24 hours after α-syn PFFs application to OPCs. The scale bar represents 10 μm.

(F) The alteration of cathepsin D activity in OPCs 24 hours after α-syn PFFs application is shown. Each enzymatic activity is indicated by the initial reaction velocity (% of control velocity), which was calculated from the change of relative fluorescence units (RFU) during the first 5 minutes of the reaction. Mean±SEM; n=5, respectively; independent cultures; one-way ANOVA. **$p<0.01$, ***$p<0.001$.

(G) (H) LDH as well as WST activity in culture medium indicates that α-syn PFFs application does not induce acute cell death in OPCs or OLGs during a time frame of 24 hours. Mean±SEM; n=5, respectively; independent cultures.

(I) (J) Quantitative real-time PCR analysis shows mRNA expression of *Gdnf* and *Igf-1* in α-syn PFFs (3 μM)-treated oligodendrocyte lineage cells. Mean±SEM; n=6, respectively; independent cultures; paired t-test, *$p<0.05$.

(K) (L) (M) RNA-seq analysis of α-syn PFFs-treated OPCs reveals altered expression of transcripts related to (K) proteolysis and protein trafficking, (L) phenotypic markers, and (M) risk genes for familial Parkinson's disease and MSA. Each pair of OPC culture samples (OPC1, OPC2, and OPC3) was allocated for the two groups with and without α-syn PFFs (3 μM) application.

Supplemental Figure S4

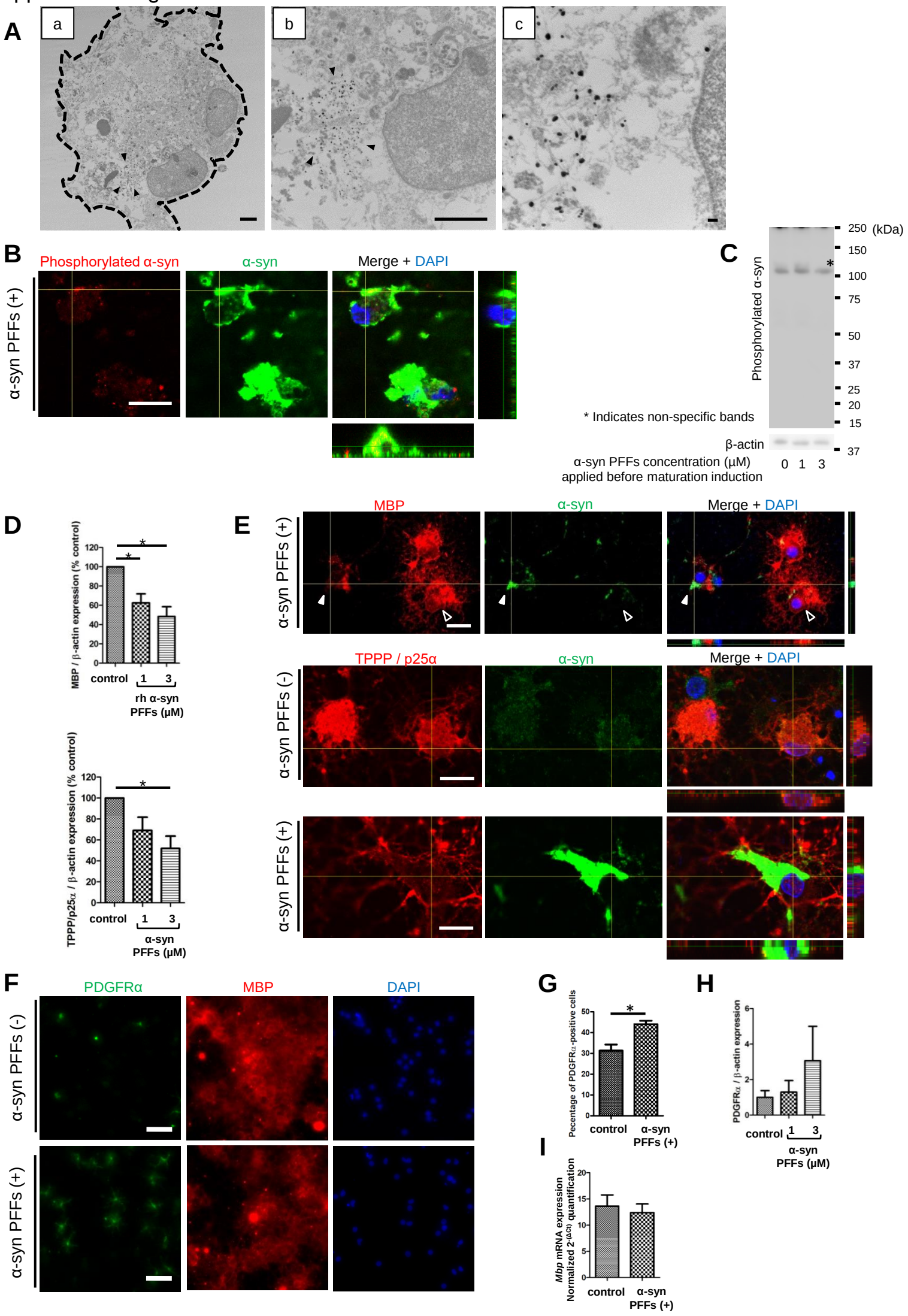

Figure S4 Decreased Expression of Myelin-associated Proteins in OLGs Derived from α-Syn PFFs-treated OPCs

(A) Immunoelectron microscopy of mature OLGs differentiated from α-syn PFFs (1 μM)-pretreated OPCs shows intracellular localization of fibrillary α-syn. The primary antibody recognizes both rat and human α-syn. a),b) Immunogold labeling of α-syn in OLGs shows intracellular α-syn localization (arrow heads). The scale bar represents a) 2 μm and b) 500 nm, respectively. The cell membrane is traced with dotted lines. c) Magnified image of gold particles associated with fibril-like structures adjacent to the nucleus. The scale bar represents 100 nm.

(B) (C) α-Syn aggregates in OLGs derived from α-syn PFFs-treated OPCs are vaguely immunoreactive to phosphorylated α-syn antibody (B). The scale bar represents 20 μm. The expression of phosphorylated α-syn is, however, not clearly confirmed by immunoblot analysis (C).

(D) Quantification by immunoblot analysis in OLGs derived from α-syn PFFs-treated OPCs shows significant reductions of MBP and TPPP/p25α protein expression. Mean±SEM; n=4, respectively; independent cultures; one-way ANOVA, *$p<0.05$.

(E) Confocal microscopy reveals that MBP expression in OLGs containing α-syn aggregates is markedly decreased (white arrow heads) in contrast to OLGs not containing aggregates (void arrow heads). The scale bar represents 20 μm. TPPP/p25α expression is also affected by α-syn PFFs application. Each scale bar represents 20 μm.

(F) Distribution of cells labeled with PDGFRα and MBP is shown. OLG culture derived from α-syn PFFs (1 μM)-treated OPCs contains more PDGFRα-positive cells, compared with normal OLG culture. Each scale bar represents 50 μm.

(G) Quantification of the percentage of PDGFRα-positive cells suggests the inhibition of OLG maturation due to α-Syn PFFs (1 μM) application. Mean±SEM; n=3, respectively; independent cultures; paired t-test, *$p<0.05$.

(H) Quantification of immunoblot analysis of OLG culture derived from α-syn PFFs-treated OPCs shows increasing trend of PDGFRα protein expression (normalized by β-actin expression). Mean±SEM; n=4, respectively; independent cultures; paired t-test.

(I) Quantification of *Mbp* mRNA expression in these OLGs reveals downward trend of *Mbp* gene expression induced by α-syn PFFs (3 μM) application. Mean±SEM; n=4, respectively; independent cultures; paired t-test.

Supplemental Movie S1 Time-Lapse Video of Primary OPC Culture Incubated with Proliferation Medium

Primary OPC culture was incubated for 62 hours with proliferation medium containing PDGF-AA and FGF-2. Images were acquired at defined positions every 10 minutes.

Supplemental Movie S2 Time-Lapse Video of Primary OPC Culture Incubated with Differentiation Medium

Primary OPC culture was incubated for 62 hours with differentiation medium containing CNTF and T3. Images were acquired at defined positions every 10 minutes.